Discrete-time switching state-space controller of DC drive

GRZEGORZ SIEKLUCKI, BARBARA BISZTYGA, RAJMUND SYKULSKI, ANTONI ZDROJEWSKI
and TADEUSZ ORZECHOWSKI

Control synthesis with state variables constraints for the DC drive is considered. Constraints are defined for the specific operating states of the DC motor during starting and braking in the presence of selected specific conditions. The control signal is based on the reference values and current state of the motor. The inverse dynamics method is applied. Closed-loop control law is realized by means of switching state-space controller.

Key words: DC drive, state variable constraints, switching gain matrix controller, state variables controller

1. Introduction

Most of the real processes are subject to certain restrictions. They are natural consequences of the limited resources of energy and how it is processed, the construction of devices, actuators and also the environmental conditions. In real dynamic systems state and control variables are constrained due to technical and energy reasons. In drive systems with electrical motors such values as maximum current in electrical circuits, derivatives of currents, shaft velocities and power supplied to the system are usually limited.

In the control theory, such constraints can be defined in many ways: as lower/upper limits (boundary layer) of the signals, boundary conditions of variables or trajectories in the state space. Moreover, these constraints can also express our expectations that the control system has to be satisfied. Hence, they are defined as the main content of the control tasks, which goal is tracking of desired trajectory. Constraints are met in the optimization problems, where decision variables subject to restrictions. They can be also described as signal limits by the saturation elements (e.g. conventional PID controllers). The problems with constraints take place in several areas of control theory

The Authors are with AGH University of Science and Technology, Faculty of Electrical Engineering, Automatics, Computer Science and Biomedical Engineering Al. Mickiewicza 30, 30-059 Krakow, Poland. E-mails: sieklo@agh.edu.pl, bisztyga@agh.edu.pl, sykulski@agh.edu.pl, zdrojton@agh.edu.pl, orzech@agh.edu.pl

such as optimization, adaptation, variable structure control and also in inverse dynamics problems [1, 3, 7, 27, 28].

The control synthesis of the DC drive can be defined as the optimal-energy control, LQ problem [5, 12], control selection for starting and stabilization [4, 13, 14, 26], sliding mode control [7, 9, 27], motor torque control [21, 23] and also in cascade control structure [11, 20].

Furthermore, the control synthesis of the DC drive is considered. It is assumed that the DC drive system will realize the reference current curve. This current curve involve all the constraints that arise from operating conditions of the DC drive. To solve this problem inverse dynamics methodology will be used. The control system structure resulting from carried out studies is presented in Figure 1.
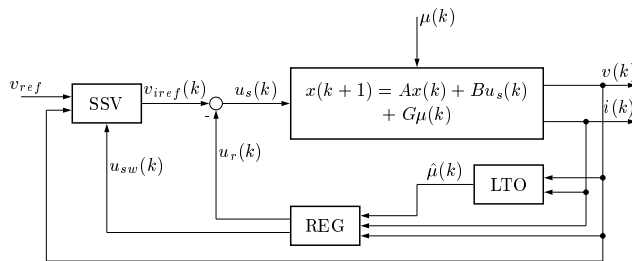

Figure 1. Control system structure

The paper is organized as follows. At first, the discrete-time control based on inverse dynamics is briefly outlined. Then, mathematical model of the DC drive and its constraints of the state variables are presented. Next, switching-gain controller is discussed in detail. Both, the starting and braking problems, are solved in three stages. The stabilization of the angular velocity at variable load torque is treated as the additional independent fourth stage which is not further discussed. The rest part of the work is devoted to both experimental and simulation researches of the selected DC drive. Some conclusions resulting from carried out practical and theoretical studies are mentioned at the end of the paper.

2.   Discrete-time control of dynamic system with state variables constraints

In this section basic problems of inverse dynamics are presented. For the purpose of control synthesis discrete-time dynamic model of a plant in state-space domain is taken into account. The mathematical model of a plant is considered

$$x(k+1) = Ax(k) + Bu(k), \qquad x(0) = x_0 \qquad (1)$$

where

$$
x(k) = \begin{pmatrix} x_1(k) \\ x_2(k) \\ \vdots \\ x_p(k) \\ \vdots \\ x_n(k) \end{pmatrix} \in \mathbb{R}^n, \; u(k) = \begin{pmatrix} u_1(k) \\ u_2(k) \\ \vdots \\ u_l(k) \\ \vdots \\ u_m(k) \end{pmatrix} \in \mathbb{R}^m, \tag{2}
$$

Solution of the equation (1) is given as

$$
x(k) = A^k x(0) + \sum_{j=0}^{k-1} A^{k-j-1} Bu(j) \tag{3}
$$

The $\mathscr{Z}$ transformation of (1) is of the form (4)

$$
z\hat{x}(z) - zx(0) = A\hat{x}(z) + B\hat{u}(z) \tag{4}
$$

that is the basis for direct determination of the state-space controller.

The *inverse dynamics problem* consists in the control signals calculation for previous defined reference state variables. Hence, the control $u(k)$ results directly from the solution of the equation (3) or (4).

Inverse dynamics is realizable when invertibility of the input-output system dynamics is possible and system is minimum phase i.e. its input-output transfer function has all zeros inside unit circle in the complex plane.

The notion of *connection of state variables with control* is helpful.

Definition 1 *For state-space equation* (1) – (2) *the state variable with index p is **connected** with the input of the system* (1) *with index l if the control $u_l(k)$ affects $x_p(k)$.*

Theorem below is useful in solving the inverse problem and it is an extension of the continuous-time method presented in [18].

Theorem 13 *Control along state variable constraints for multivariable systems. If the dynamic system* (1) *is controllable and m $\mathscr{Z}$ transformations of the state vector $\hat{x}(z)$ are known (functions satisfying state variables constraints) and each of these functions is connected with another control signal, then the $\mathscr{Z}$ transformation of the control vector $\hat{u}(z)$ can be calculated on the basis of the equation*

$$
B\hat{u}(z) = (zI - A)\hat{x}(z) - zx(0) \tag{5}
$$

where x(0) is an initial condition.

This theorem states the conditions for the solvability of inverse problem.

The control $u(k)$ carrying out the system along constraints of the state variables is performed as follows: at first, $\mathscr{Z}$ transformations of constraints are calculated, next $\hat{u}(z)$ from (5) is achieved and eventually control $u(k)$ in the time domain is obtained by inverse $\mathscr{Z}$ transform of $\hat{u}(z)$.

Comments on Theorem 13

(i) The assumption concerning the number of constraints functions and their connection with control vector result from the condition of the solution (5).

(ii) The equation (5) is the system of n-polynomial equations where m components of vector $\hat{u}(z)$ and $n - m$ unknown functions of the state vector $\hat{x}(z)$ which fully describes the system trajectory have to be determined.

(iii) The $u(k)$ is the control signal in open-loop system but it is possible to determine $u(k)$ as the feedback signal from state vector $x(k)$.

3.   Mathematical model of the DC drive and its state variable constraints

Mathematical model of the separately excited DC motor according to [10, 11, 15, 16, 20, 22] alongside the power actuator model can be described by the following state space equation

$$
\begin{pmatrix} \dot{\omega}(t) \\ \dot{I}(t) \end{pmatrix} = \begin{pmatrix} 0 & \psi_e/J \\ -\psi_e/L & -1/T \end{pmatrix} \begin{pmatrix} \omega(t) \\ I(t) \end{pmatrix} + \begin{pmatrix} -1/J & 0 \\ 0 & K_p/L \end{pmatrix} \begin{pmatrix} M_m(t) \\ U_s(t) \end{pmatrix}
\tag{6}
$$

where: U_s – voltage control of the power actuator, I – armature current, M_m – load torque, ω – angular velocity, ω_0 – nominal no-load speed, ψ_e – flux linkage, T_m – starting electromechanical time constant, T – electromagnetic time constant, J – moment of inertia, B – electromechanical time constant, R – generalize resistance, L – total armature inductance, K_p – gain of power actuator.

The mathematical model (6) is valid in the following assumptions: the power actuator is an inertialess system with constant gain K_p (this assumption is satisfied for modern power converters e.g. [8, 19]), drive works in range of continues current, commutation process does not influence on external measurable parameters of drive. Those assumptions do not limit the use of (6) because they are always satisfied for drive systems with properly taken motor and power actuator.

A DC drive system properly working in a dynamical states has the current (motor torque) constraints:

$$
\left\{ \begin{array}{ll} |I(t)| \leqslant I_d = \lambda I_N & \text{– current value constraint,} \\[2mm] \left| \dfrac{dI(t)}{dt} \right| \leqslant p I_N & \text{– current derivative constraint} \end{array} \right\}
\tag{7}
$$

where λ, p are positive definite constants and the subscript $_N$ means nominal (rated) value.

In the following researches the dynamical model (6) in per units values (p.u.) is taken into account:

$$u_s(\tau) = \frac{K_p U_s(t)}{U_N}, \quad i(\tau) = \frac{I(t)}{I_N}, \quad a = \frac{T_m}{T},$$

$$B = J\frac{R}{\psi_e^2}, \quad v(\tau) = \frac{\omega(t)}{\omega_0}, \quad T_m = J\frac{\omega_0}{M_N} = Bh, \tag{8}$$

$$\mu(\tau) = \frac{M_m(t)}{M_N}, \quad \tau = \frac{t}{T_m}, \quad h = \frac{U_N}{I_N R}.$$

Inserting (8) into model (6) the following state equation of DC drive is obtained

$$\dot{x}(\tau) = \widetilde{A}x(\tau) + \widetilde{B}u(\tau) \tag{9a}$$

where

$$u(\tau) = \begin{pmatrix} \mu(\tau) \\ u_s(\tau) \end{pmatrix}, \qquad x(\tau) = \begin{pmatrix} v(\tau) \\ i(\tau) \end{pmatrix}, \tag{9b}$$

$$\widetilde{A} = \begin{pmatrix} 0 & 1 \\ -ah & -a \end{pmatrix}, \qquad \widetilde{B} = \begin{pmatrix} -1 & 0 \\ 0 & ah \end{pmatrix} \tag{9c}$$

The constraints (7) take a new form:

$$|i(\tau)| \leqslant \lambda \tag{10}$$

$$\left|\frac{di(\tau)}{d\tau}\right| \leqslant j_d = pT_m \tag{11}$$

The synthesis of the controller can be performed using discrete time mathematical model of the electrical drive. The ZOH discretization method is preferred because discrete-time controllers with AD converters are most frequently used.

The model (9) after discretization process with ZOH is described by the difference equation [20]

$$x(k+1) = Ax(k) + Bu_s(k) + G\mu(k) \tag{12}$$

where

$$A = \begin{pmatrix} a_{11} & a_{12} \\ a_{21} & a_{22} \end{pmatrix}, B = \begin{pmatrix} b_1 \\ b_2 \end{pmatrix}, G = \begin{pmatrix} g_1 \\ g_2 \end{pmatrix}, \tag{13}$$

$$a_{21} = -aha_{12}$$

This model will be used in the control synthesis.

4.   Synthesis of switching state-space controller

Fully performed control synthesis requires consideration of several characteristic work conditions of DC drive i.e. starting, braking, stabilization.

In general, the control $u(k)$ is in the following form

$$u_i(k) = -K_i x(k) + v_{i\,ref}(k) \tag{14a}$$

where K is the feedback matrix gain

$$K_i = \begin{pmatrix} k_{i1} & k_{i2} \end{pmatrix} \tag{14b}$$

Starting of DC drive

For continuous mathematical model (in p.u.) of DC motor (9) and constraints (10), (11) optimum start-up curve is shown in Fig. 2 [18].
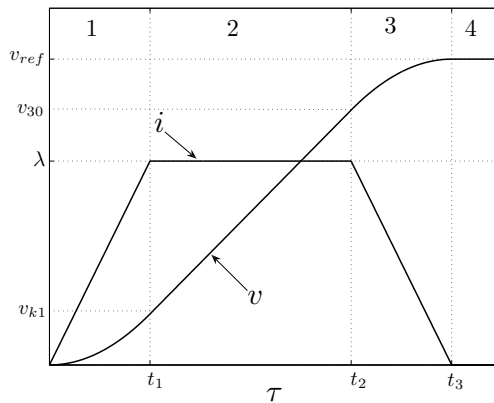

Figure 2. Armature current and angular velocity during the starting $\mu = 0$

Starting of the motor consists of 3 segments of current function:

1. linear function – constraint (11) takes place

$$i_1(\tau) = j_d \tau \quad \tau \in [0, t_1] \tag{15}$$

2. constant function with constraint (10)

$$i_2(\tau) = \lambda \quad \tau \in (t_1, t_2] \tag{16}$$

3. linear function – constraint (11) takes place again

$$i_3(\tau) = -j_d\tau + \lambda \quad \tau \in (t_2, t_3] \tag{17}$$

$\mathscr{L}$ transform is calculated for each segment of the starting curve (T_s is a sampling time):

$$i_1(k) = j_d T_s k \qquad \xrightarrow{\mathscr{L}(\cdot)} \frac{j_d T_s z}{(z-1)^2} = \hat{i}_1(z), \tag{18}$$

$$i_2(k) = \lambda \qquad \xrightarrow{\mathscr{L}(\cdot)} \frac{\lambda z}{z-1} = \hat{i}_2(z), \tag{19}$$

$$i_3(k) = -j_d T_s k + \lambda \xrightarrow{\mathscr{L}(\cdot)} \frac{\lambda z^2 - (j_d T_s + \lambda)z}{(z-1)^2} = \hat{i}_3(z). \tag{20}$$

The mathematical model (12) is considered for vector G equals 0 but $b_2 \neq 0$.

The control $u(k)$ is evaluated independently for each segment. Each stage begins in the new time, taking $k = 0$. The control problem is calculated for the new initial state x_0. The result of the calculations is a sequence of three matrices $\{K_1, K_2, K_3\}$ of the controller.

Stage 1: Initial conditions are

$$i_{10} < \lambda, \quad v < v_{30} \tag{21}$$

These values are marked in the figure 2.

Inserting (18) and (21) to equation (12) the $\mathscr{L}$ transform of control signal is obtained in the following form

$$\hat{u}_s^1(z) = -\frac{a_{21}}{b_2}\hat{v}_1(z) - \frac{a_{22}}{b_2} \cdot \frac{j_d T_s z}{(z-1)^2} + \frac{j_d T_s z^2}{b_2(z-1)^2} \tag{22}$$

and after inverse $\mathscr{L}$ transform control signal in sampling domain is

$$u_s^1(k) = -\frac{a_{21}}{b_2}v_1(k) - \left(\frac{a_{22}-1}{b_2}\right)j_d T_s k + \frac{j_d T_s}{b_2} \tag{23}$$

Thus,

$$u_s^1(k) = -K_1 x(k) + v_{1ref}(k) \tag{24a}$$

where

$$k_{11} = \frac{a_{21}}{b_2}, \quad k_{12} = \frac{a_{22}-1}{b_2}, \quad v_{1ref}(k) = \frac{j_d T_s}{b_2} \tag{24b}$$

Stage 2: In this case initial conditions equal

$$i_{20} = \lambda, \quad v < v_{30} \tag{25}$$

As in the first stage the control law is in the following form

$$u_s^2(k) = -K_2 x(k) + v_{2ref}(k) \tag{26a}$$

where

$$k_{21} = \frac{a_{21}}{b_2}, \quad k_{22} = 0, \quad v_{2ref}(k) = \lambda \left(\frac{1 - a_{22}}{b_2} \right) \tag{26b}$$

Stage 3: Initial conditions are

$$i_{30} \leqslant \lambda, \quad v \geqslant v_{30} \tag{27}$$

and initial angular velocity:

$$
\begin{aligned}
v_{30} &= v_{ref} - \triangle v_3(k) \\
&= v_{ref} + \frac{(\mu - \lambda)(a_{cl12}\lambda b_2 - a_{cl12}\mu b_2 - j_d T_s a_{cl12} b_2 + 2 j_d T_s b_1)}{2 j_d T_s b_2}
\end{aligned} \tag{28}
$$

where $a_{cl12} = \dfrac{aha_{12}^2 + aa_{12}a_{22} - aa_{12} + a_{22}^2 - 2a_{22} + 1}{aha_{12}}$. The condition of switch-on the third stage ($u_s^3(k)$) is $v = v_{30}$. The value (28) depends on the load torque μ.

As previously, the last control law is expressed in the following form

$$u_s^3(k) = -K_3 x(k) + v_{3ref}(k) \tag{29a}$$

where

$$k_{31} = \frac{a_{21}}{b_2}, \quad k_{32} = \frac{a_{22} - 1}{b_2}, \quad v_{3ref}(k) = -\frac{j_d T_s}{b_2} \tag{29b}$$

Moreover, the formula (13) can be written as $\frac{a_{21}}{b_2} = -1$ and thus gain matrices are in simple form

$$K_1 = K_3 = \begin{pmatrix} -1 & \dfrac{a_{22} - 1}{-a_{21}} \end{pmatrix}, \tag{30a}$$

$$K_2 = \begin{pmatrix} -1 & 0 \end{pmatrix} \tag{30b}$$

The control laws (24a), (26a) and (29a) are shown in the block structure of DC drive control system (Fig. 3)

The next stage of the control synthesis is the stabilization of the angular velocity which is not considered in this paper.

Braking of DC drive

Braking of the DC motor is carried out by using the same control gain matrices K_i as for the start-up, but all setvalues v_{iref} are multiplied by -1.

The third stage condition $v = v_{30}$ for braking process has similar form to (28)

$$v_{30} = v_{ref} - \triangle v_3 = v_{ref} + \tfrac{1}{2} a_{cl12}(\lambda + \mu) - \tfrac{1}{2} \left(\tfrac{2(\lambda + \mu)b_1}{b_2} + \tfrac{(\lambda + \mu)^2 a_{cl12}}{j_d T_s} \right) \tag{31}$$

Synthesis results allow to construct the control system structure (Fig. 1).

5.   Control system structure

The function of the controller REG is simultaneous switching of the gain matrix controller K_i and selecting of setvalue v_{iref} depending on actual state vector in the suitable stage: starting, braking or stabilization of the drive. The control $u_r(k)$ and the decision $u_{sw}(k)$ are the REG output signals. The REG makes decision on signal $u_{sw}(k)$ independently in every stage.
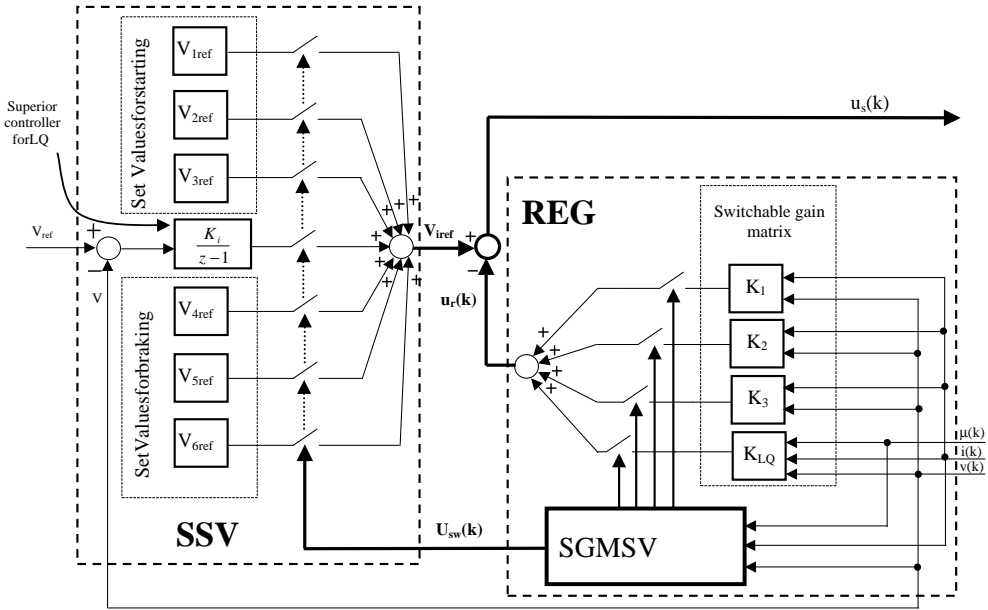

Figure 3. Structure of DC drive control system

The structure of the proposed control system is presented in Fig. 3. The block selection SSV of the setpoint and REG unit are emphasized. The sequence of the gain matrix feedback controller $K_i = \{K_1, K_2, K_3\}$ is provided by control synthesis. Then the setpoints $v_{iref} = \{v_{1ref}, v_{2ref}, v_{3ref}, v_{4ref}, v_{5ref}, v_{6ref}\}$ are calculated respectively. The switching conditions $u_{sw}(k)$, for every gain matrix K_i with assigned setpoints are the final goal of the control synthesis. This task is performed by SGMSV block.

During the executing of the control task only one connector in REG unit and SSV unit is turned on.

The controller is the state-variable feedback controller. Load Torque Observer (LTO) should be applied (what is shown in Fig. 1).

6.   Practical results

Practical tests have been carried out and the results obtained make the correction of quality control possible (i.e. precision of current curve tracking).

The control system from Fig. 3, with sampling time $T_s = 0.0005$s, is realized in Simulink with Real-Time Workshop Toolbox. The parameters of the drive system and the power converter used in researches are included in the Appendix.

Results are shown in Fig. 4, 5 and 6 for different values ω_{ref}, R, λ. The drive system starts from the point of equilibrium equals zero and without the load torque.
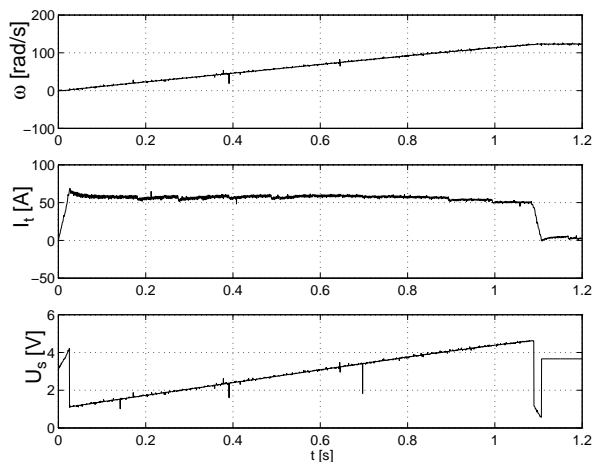
Figure 4. Drive starting ($\omega_{ref} = 120[rad/s]$, $\lambda = 1.0$, $R = 1.2[\Omega]$ in calculations)

In general, in stage 2 with flat current curve, the control signal gives wrong results (current exceeds the constraints (7)), because of the lack of feedback signal from the armature current ($k_{22} = 0$). Thus, the control signal (26a) should be supplemented by the corrector $f(\lambda - i)$ and then

$$u_s^2(k) = -K_2 x(k) + v_{2ref}(k) + f(\lambda - i) \tag{32}$$

Function f can be chosen as $sgn(K_2^1(\lambda - i))$ or $sat(K_2^1(\lambda - i))$. The first case may generated chattering [27] (it will not be used). In the second case, for $K_2^1 = 3$ and saturation equals ± 1, improved results are presented in the figure 6. Moreover, the reference angular velocity is achieve without the overshoot.

The results are consistent with the reference current curve in the figure 2. Thus, this method with corrector (32) can be implemented in the real-time in practice.
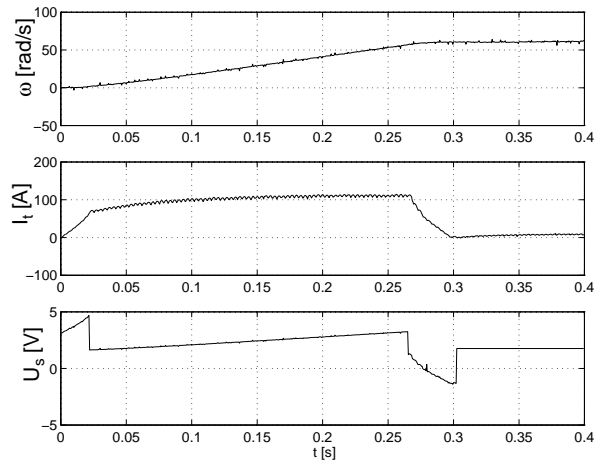
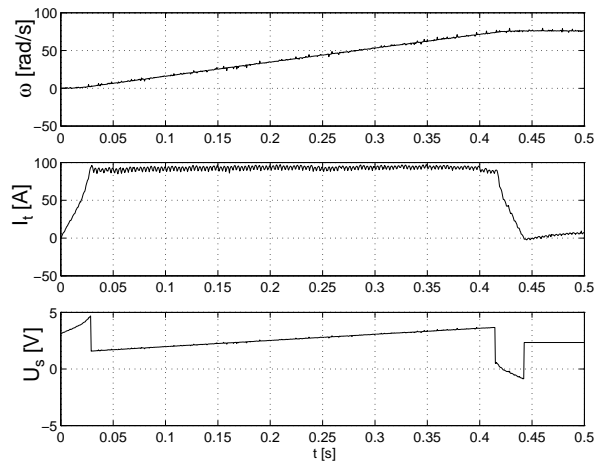Figure 5. Drive starting ($\omega_{ref} = 60[rad/s]$, $\lambda = 2.0$, $R = 2.3[\Omega]$ in calculations)

Figure 6. Drive starting ($\omega_{ref} = 80[rad/s]$, $\lambda = 2.0$, $R = 2.3[\Omega]$ in calculations)

7. Simulations of the load torque influence on motor starting

Simulation researches have been performed in Matlab-Simulink software environment for the following parameters: integration method with fixed stepsize equals 0.00002 [s], sampling time of the control system $T_s = 0.0005[s]$, time constant of the load torque observer $T_a = 0.002[s]$ (which is presented in appendix eqn. (33)). The particular states of the DC motor, during starting, have been verified for step load torques in different

points of time. Simulation results are presented in the form of state variables ω, I and the switching signal of the state controller u_{sw} plots.

The figure 7 concerns three types of the motor starting:

- line 1 - start from $\omega(0) = 0[rad/s]$, $I(0) = 0[A]$, $M_m(0) = 0[Nm]$,

- line 2 - start from $\omega(0) = 0[rad/s]$, $I(0) = 0[A]$, $M_m(0) = 80[Nm]$,

- line 3 - start from $\omega(0) = 60[rad/s]$, $I(0) = 18[A]$, $M_m(0) = 40[Nm]$.

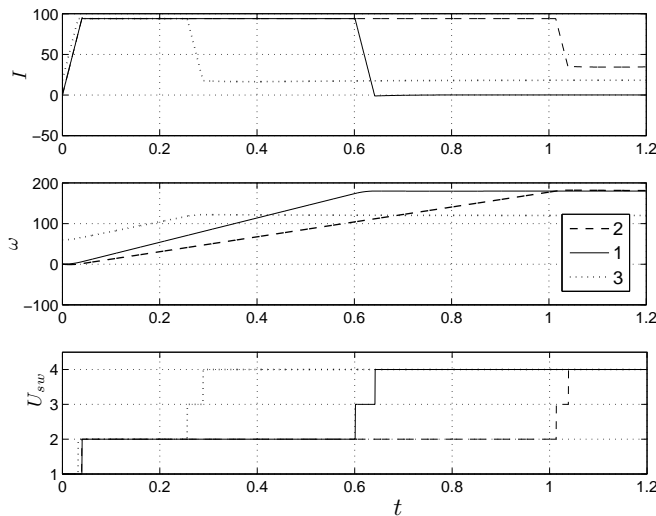Presented curves confirm the effectiveness of the applied method in terms of the state variables constraints.

Figure 7. DC drive starting for different reference values: line 1 and 2 – $\omega_{ref} = 180[rad/s]$, line 3 – $\omega_{ref} = 120[rad/s]$.

Figures 8 and 9 refer to the start-up with no-load at time $t = 0[s]$, but the step of load torque takes place in several points of time:

- line 4 - impact load in stage 1, i.e. $M_m(t) = 80 \cdot \mathbf{1}(t - 0.01)$,

- line 5 - impact load in stage 2, i.e. $M_m(t) = 80 \cdot \mathbf{1}(t - 0.2)$,

- line 6 - impact load in stage 3, i.e. $M_m(t) = 80 \cdot \mathbf{1}(t - 0.61)$,

The same curves (4, 5, 6) are placed on the enlargement scale in figure 9.

The points at which the motor current decreases and the points of maximum overshooting of the angular velocity are shown. In the current curve in the stage 3 one oscillation is visible. This effect results from inertial response of the load torque observer.
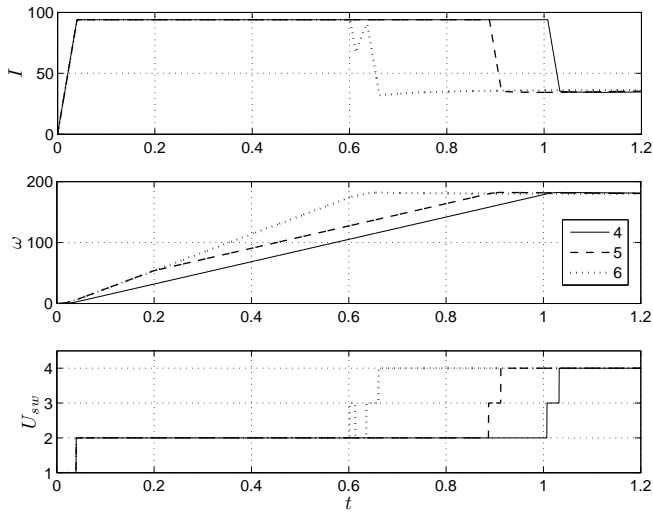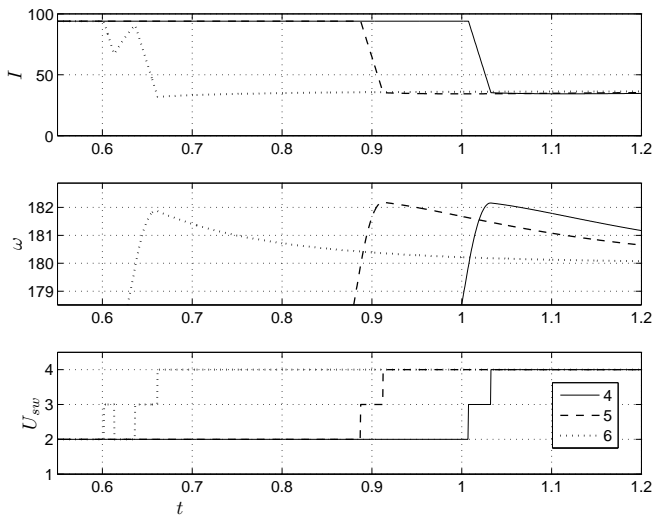
Figure 8. DC drive starting with load torque

Figure 9. Switching from the 2nd to the 3rd stage.

In the last figure (fig. 10) line number 6 is repeated and two additional lines (7 and 8) for two different time constants T_a of the load torque observer are presented. There is the upper limit of the T_a for which the observer works fast enough and the current curve does not exceed the current selected constraints.
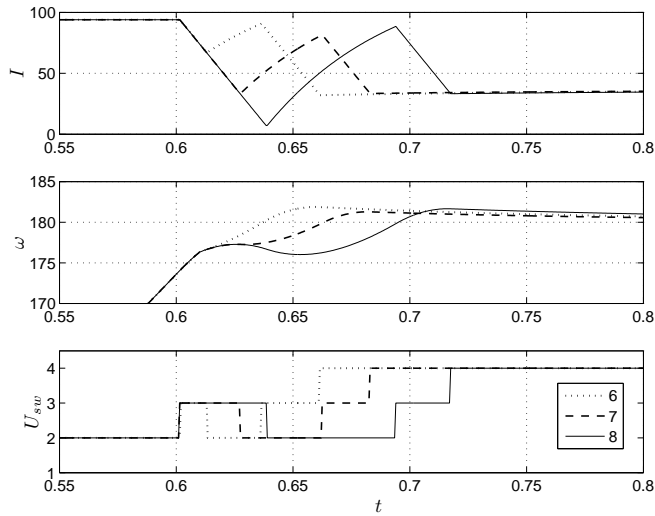
Figure 10. Influence T_a of load torque observer on current curve: line 6 - $T_a = 2[ms]$, line 7 - $T_a = 10[ms]$, line 8 - $T_a = 19.8[ms]$.

Carried out simulation researches prove that proposed start-up system is insensitive to varying duty. The proposed start-up system works well.

8.   Conclusion

The presented method can be implemented, as supervisory control, in electrical drive systems where the mathematical model of the motor torque is linear. Thus, this method can be also used in the following systems [22]:

- PMSM drives (in rotor flux frame coordinates),

- squirrel cage induction motors in rotor field oriented control systems.

The greatest advantage of this method is independence from the type of model plant, no matter if a motor is the inertia or oscillatory element:

- big value of J – the drive system is at least a 2nd order inertia element,

- small value of J – the drive system is probably an oscillatory element, at least 2nd order.

Concluding, the control problem under the linear-switchable constraints for linear dynamical system has been resolved. The inverse dynamics method has been confirmed

experimentally. Practical researches have been performed for the nonlinear and uncertain system [24] such as the DC motor with thyristor power converter. The simulation researches for the similar control system have been carried out, too, in which the load torque influence on the reference current curve realization has been investigated. In general, theoretical results have been verified.

Stability analysis of the presented system is complicated because of the mathematical model uncertainty, quantization process and sampling time (uncertain sampled-data control system). This problem requires further detailed analysis.

9. Appendix

9.1. Drive parameters

$$P_N = 18[\text{kW}], \qquad U_N = 440[\text{V}], \qquad I_N = 47[\text{A}],$$
$$\psi_{eN} = 2,197[\tfrac{\text{Vs}}{\text{rad}}], \quad \omega_N = 188[\tfrac{\text{rad}}{\text{s}}], \quad \omega_0 = 200,3[\tfrac{\text{rad}}{\text{s}}],$$
$$J = 0,69[\text{kgm}^2], \quad R = 1,8[\Omega], \qquad L = 99[\text{mH}],$$
$$K_p = 75[\tfrac{\text{V}}{\text{V}}], \qquad p = 50[\tfrac{\text{A}}{\text{s}}], \qquad \lambda_N = 2[\tfrac{I_{max}}{I_N}]$$

9.2. Load Torque Observer

There are different kinds of the state variable observers like: linear, nonlinear, sliding mode, full or reduced order [1, 2, 6, 14, 17, 25].

The continuous-time Load Torque Observer can be designed as [25]

$$\hat{M}_m(s) = \frac{\psi_e}{(T_a s + 1)^2} I(s) - \frac{Js}{(T_a s + 1)^2} \omega(s) = G_1(s)I(s) - G_2(s)\omega(s). \qquad (33)$$

where T_a is the time constant.

After discretization with zero order hold element the observer is obtained in the following form

$$\hat{M}_m(z) = \frac{z-1}{z} \cdot \left(\mathscr{Z}\left[\mathscr{L}^{-1}\left\{ \frac{G_1(s)}{s} \right\} \right] I(z) - \mathscr{Z}\left[\mathscr{L}^{-1}\left\{ \frac{G_2(s)}{s} \right\} \right] \omega(z) \right) \qquad (34)$$

where $\mathscr{Z}$ is **Z**-transform and $\mathscr{L}^{-1}$ is inverse Laplace transform. The observer (34) has been verified in practice.

References

[1] K.J. ÅSTRÖM and B. WITTENMARK: Adaptive Control. Reading, Addison-Wesley, 1995.

[2] K.J. ÅSTRÖM and B. WITTENMARK: Computer-Controlled Systems. NJ: Prentice Hall, 1997.

[3] B.D.O. ANDERSON and J.B. MOORE: Optimal control: Linear Quadratic methods. Englewood Cliffs, NJ: Prentice Hall, 1990.

[4] J. BARANOWSKI, M. DŁUGOSZ, M. GANOBIS, P. SKRUCH and W. MITKOWSKI: Applications of mathematics in selected control and decision processes. *Matematyka Stosowana (Mathematica Applicanda)*, **12**(53), special issue, (2011), 65-90.

[5] J. BARANOWSKI, M. DŁUGOSZ and W. MITKOWSKI: Remarks about DC motor control. *Archives of Control Sciences*, **18**(3), (2008), 289-322.

[6] G. BARTOLINI, L. FRIDMAN, A. PISANO and E. USAI: Modern Sliding Mode Control Theory: New Perspectives and Applications. Berlin , Springer-Verlag, 2008.

[7] A. BARTOSZEWICZ: Sliding mode control systems with time-varying switching surfaces. Zeszyty Naukowe. Rozprawy Naukowe. Lodz University of Technology, 2000, (in Polish).

[8] M. BASZYŃSKI: A model of the three-phase bridge rectifier with sinusoidal source current using fpga implementation. *Przeglad Elektrotechniczny*, **85**(3), (2009), 36-41.

[9] B. BISZTYGA and G. SIEKLUCKI: Sliding mode control of the DC drive with relative degree higher than one. *Przeglad Elektrotechniczny*, **88**(11a), (2012), 38-42.

[10] K. BISZTYGA: Control of electrical drives. *Sterowanie i regulacja silników elektrycznych*. Warszawa, WNT, 1989, (in Polish).

[11] A. CIEPIELA: Automation of Converter-based DC drive. Kraków, Wydawnictwa AGH, 1992, (in Polish).

[12] M. DŁUGOSZ: Minimal energy control of DC motor. *Prace Naukowe Politechniki Slaskiej. Elektryka*, **1** (2011), 89-98.

[13] M. DŁUGOSZ: Optimization problems of power transmission in automation and robotics. *Przeglad Elektrotechniczny*, **87**(9a), (2011), 238-242.

[14] M. DŁUGOSZ: Optimization problems of drive systems in automation and robotics. Wydawnictwa Naukowe AGH Krakow, 2012, (in Polish).

[15] M.P. KAŹMIERKOWSKI and H. TUNIA: *Automatic Control of Converter-Fed Drives*. Amsterdam, ELSEVIER, 1994.

[16] W. LEONHARD: *Control of Electrical Drives*. Berlin, Springer-Verlag, 1997.

[17] T. ORŁOWSKA-KOWALSKA: Sensorless Induction Motor Drives. Wroclaw University of Technology Press, 2003, (in Polish).

[18] T. ORZECHOWSKI and G. SIEKLUCKI: Control of Dynamic System with State Variables Constraints, Applied to DC Drive. *SAMS*, **38** (2000), 601-620.

[19] A. PENCZEK, R. STALA, Ł. STAWIARSKI and M. SZAREK: Hardware-in-the-loop FPGA-based simulations of switch-mode converters for research and educational purposes. *Przeglad Elektrotechniczny*, **87**(11), (2011), 194-200.

[20] G. SIEKLUCKI: Automation of the drive. Krakow, Wydawnictwa AGH, 2009, (in Polish).

[21] G. SIEKLUCKI: Pole placement method for DC motor torque controller. *Archives of Control Sciences*, **19**(3), (2009), 307-324.

[22] G. SIEKLUCKI: Analysis of the transfer-function models of electric drives with voltage controlled source. *Przeglad Elektrotechniczny*, **88**(7a), (2012), 250-255.

[23] G. SIEKLUCKI: Loopshaping of motor torque controller. *Archives of Control Sciences*, **23**(2) (2013), 213-228.

[24] G. SIEKLUCKI and B. BISZTYGA: Uncertainty mathematical models of power converters. *Automatyka*, ISSN 1429-3447, **13**(1), (2012), 73-87.

[25] G. SIEKLUCKI and T. ORZECHOWSKI: Discrete-time load torque observers in electric drives. *Automatyka*, ISSN 1429-3447, **14**(1), (2010), 113-132, (in Polish).

[26] G. SIEKLUCKI, M. TONDOS and A. PRACOWNIK: Variable structure control method of a two-mass drive system. *Elektrotechnika i Elektronika*, **26**(1-2), (2007), 69-78, (in Polish).

[27] V. UTKIN, J. GULDNER and J. SHI: Sliding Mode Control in Electromechanical Systems. London, Taylor & Francis, 1999.

[28] J.R. VACCARO: Digital Control. A State-Space Approach. Mc Graw-Hill, Inc., 1995.